EUROFUSION WPPMI-PR(16) 12773

C Reux et al.

DEMO reactor design using the new modular system code Sycomore

Preprint of Paper to be submitted for publication in
Nuclear Fusion

This work has been carried out within the framework of the EUROfusion Consortium and has received funding from the Euratom research and training programme 2014-2018 under grant agreement No 633053. The views and opinions expressed herein do not necessarily reflect those of the European Commission.

DEMO reactor design using the new modular system code Sycomore

C. Reux[1], L. Di Gallo[1], F. Imbeaux[1], J.-F. Artaud[1], P. Bernardi[1], J. Bucalossi[1], G. Ciraolo[1], J.-L. Duchateau[1], C. Fausser[2], D. Galassi[1,3], P. Hertout[1], J.-C. Jaboulay[2], A. Li-Puma[1], B. Saoutic[1], L. Zani[1], ITM-TF contributors ‡

[1]CEA, IRFM, F-13108 Saint-Paul-lez-Durance, France
[2]CEA, DEN, Saclay, DM2S, SERMA, F-91191 Gif-sur-Yvette, France
[3]Aix Marseille Université, CNRS, Centrale Marseille, M2P2 UMR 7340, 13451, Marseille, France

E-mail: cedric.reux@cea.fr

December 2014

Abstract. Demonstration power plant is the next step for fusion energy following ITER. Some of the key design questions can be addressed by simulation through system codes. System codes aim at modeling the whole plant with all its subsystems and identifying the impact of their interactions on the design choice. The SYCOMORE code is a modular system code developed to address key questions relevant for tokamak fusion reactor design. SYCOMORE is developed within the European Integrated Tokamak Modelling framework (ITM) and provides a global view (technology and physics) of the plant. It includes modules to address plasma physics, divertor physics, breeding blankets and shields design, magnet design and power balance of plant. The code is coupled to an optimization framework which allows specifying figures of merit and constraints to obtain optimized designs. Examples of pulsed and steady-state DEMO designs obtained with Sycomore are presented. Sensitivity to design assumptions are also studied, showing that the operational domain around working points can be narrow for some cases.

Introduction

The next step for fusion energy following ITER is the construction of a demonstration power plant. A viable fusion reactor aims at achieving a net electricity output together with sufficient availability, reliability at an acceptable cost. This poses major challenges on the plant design. In particular, a large number of constraints have to be met at the same time. The so-called system codes aim at addressing this design issue. They model all the subsystems in a power plant to study their interactions and their impact on the global design [1, 2, 3]. SYCOMORE is a modular system code developed to address

‡ See the Appendix to G. Falchetto et al., Nucl. Fusion 54 (2014) 043018

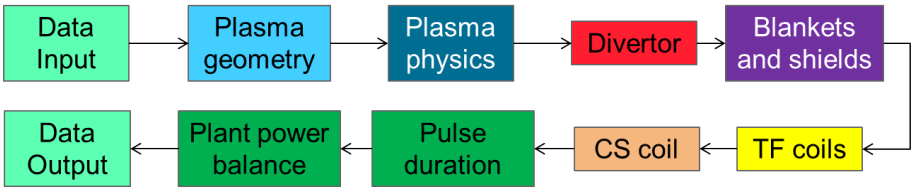

Figure 1. Sycomore code workflow - direct run mode

physics and technology issues for fusion reactors. The code was designed to be modular (giving the possibility to add new code modules), flexible (giving the possibility to update already implemented modules) and consistent (providing self-consistent designs along the calculation). The first part of the present article will describe Sycomore's computational architecture and the basic principles of the code. The second part will describe briefly the physics and technology contents of the different modules in the code. The third part of the article will show results obtained with Sycomore on two major classes of tokamak reactors: pulsed and steady-state machines.

1. General Description of the code

1.1. Code structure and calculation workflow - direct mode

Sycomore is built over a chain of code modules handling each reactor subsystem taken into account in the calculation. The modules communicate to each other using the European Integrated Tokamak Modelling framework (ITM) [4] and are chained in a graphical interface software named Kepler [5]. This allows a straightforward outlook of the calculation sequence. The present calculation chain is presented on figure 1. Sycomore can be run in two different modes: the *direct mode* and the *optimizer mode*. The direct mode is the primary way to run the code and is the one shown on figure 1. The user specifies a set of fixed inputs (among them major and minor radius, toroidal field, edge safety factor, kinetic profile parameters, etc...). These are used to compute the design and its performances (fusion power, net electric power, radial build, pulse duration etc.). No global optimization is performed at this stage. Consistency is enforced all along the calculation chain: every module checks that the data it produces is consistent with the results of module earlier in the chain. If an inconsistency is found at any point of the workflow (for instance a lack of space for any of the elements of the radial build), the calculation stops and the point is considered as invalid. This prevents inconsistent designs from being produced by the code, a situation which would require post-calculation checks. The direct mode allows quick checks of a particular design and is particularly useful for benchmarks with other system codes.

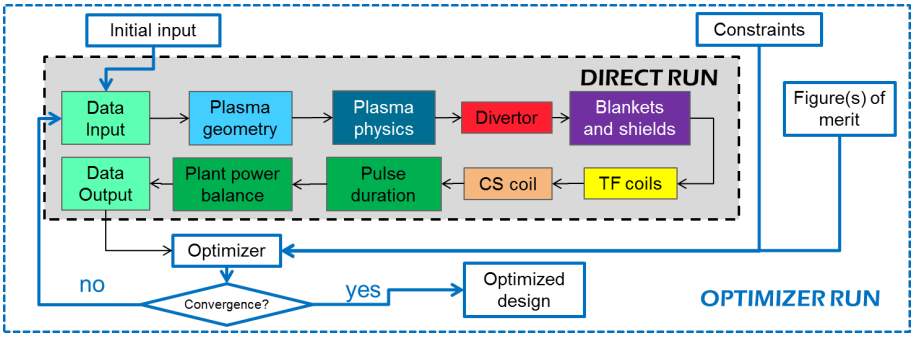

Figure 2. Sycomore code workflow - Optimier mode

1.2. Optimization mode

The second run mode of Sycomore is the *optimizer mode*. It wraps the *direct mode* workflow inside an optimizer loop (see figure 2) thus allowing the user to specify figures of merit and constraints on the design parameters. Since the core of the code is the same calculation chain as in the *direct run*, any set of input variables can be chosen as an optimization variable. All combinations of input or output variables can be chosen as figures of merit or constraints. Single-criterion problems (e.g. minimizing the major radius) or multi-criterion problems (minimizing the major radius AND maximizing the net electric power) can be solved. Multi-criterion optimizations are handled by creating Pareto fronts for the chosen problems. For the example described above, this is equivalent to find the maximum net electric power achievable for a range of major radii. Examples of single-criterion optimizer runs are presented in section 3. Multi-criterion runs are left for future work.

The URANIE [6] optimization framework developped at CEA/DEN was chosen for Sycomore. Since URANIE is an external framework, a communication library based on socket data exchange was developped. This solution keeps a maximum flexibility in the choice of the optimizer. URANIE is an uncertainty and sensitivity platform based on on the data analysis framework ROOT [7], an object-oriented petaflopic computing system developed at CERN. It provides a collection of multi-constraints multi-criterion algorithms among them genetic algorithms (GA) within the Vizir library [8] which was chosen for Sycomore. GAs use a different approach from conventional gradient-based algorithms; they are based on random processes mimicking the natural selection to evolve a population of points (or individuals) towards the optimum. A genetic algorithm proceeds in 5 steps:

(i) Evaluate the current population of individuals with the function to be optimized;

(ii) Select and rank the individuals following the figures of merit and deviations from the constraints;

(iii) Randomly recombine the individuals by pairs (with a favorable weight on best ones) to create new children. The recombination operator used in URANIE creates both heterozygotes and homozygotes individuals from the parents' genetic material.

(iv) Introduce small random changes (mutations) in the new individuals. The set of new individuals is the next generation of the population.

(v) Iterate back to the first step until the values of the function to be optimized are within a certain range for all the points of the population (i.e. a population converged on an optimum)

GAs generally need much more evaluations of the function to be optimized than classical gradient-based algorithms, but are much more robust. First of all they usually avoid the problem of being trapped in local minima of the cost function. Secondly, they are not blocked, unlike gradient-based algorithms, when encountering invalid designs, for example a set of parameters for which it is not possible to put all components in the radial build. When a design point is invalid, the GA rejects it and a new child is simply created by a recombination of other parents. This is particularly important for system codes as radial build problems can be encountered very often when exploring a large parameter space with no a priori knowledge of the valid area.

The coupling to the Optimizer framework has also been parallelized. Since all the function evaluations inside a GA generation are independent, the scaling factor is close to 100%. A typical run of Sycomore in *optimizer mode* with a population of 400 individuals requires approximately 15 min on 128 cores (for 20000 to 40000 points explored).

2. Modules content

The physics and technology content of the modules are briefly described in the present section. This is only a short summary of the main methods and assumptions used in Sycomore in order to give a global view. Some of the modules have been described in independent articles (referred to in each module's paragraph) should the reader need more details.

2.1. Plasma physics module

The plasma module is based on the Helios code [9]. It assumes parabolic profiles with a pedestal:

$$n(\rho) = \begin{cases} n_{ped} + (n_0 - n_{ped}) \left(1 - \frac{\rho^2}{\rho_{ped}^2}\right)^{\alpha_n} & \text{for } 0 \leq \rho \leq \rho_{ped} \\ n_{sep} + (n_{ped} - n_{sep}) \frac{1-\rho}{1-\rho_{ped}} & \text{for } \rho_{ped} \leq \rho \leq 1 \end{cases} \tag{1}$$

$$T(\rho) = \begin{cases} T_{ped} + (T_0 - T_{ped}) \left(1 - \frac{\rho^{\beta_T}}{\rho_{ped}^{\beta_T}}\right)^{\alpha_T} & \text{for } 0 \leq \rho \leq \rho_{ped} \\ T_{sep} + (T_{ped} - T_{sep}) \frac{1-\rho}{1-\rho_{ped}} & \text{for } \rho_{ped} \leq \rho \leq 1 \end{cases} \tag{2}$$

The pedestal temperature follows the Cordey scaling as explained in detail in [9]. Other parameteres are user inputs.

Once the profiles are known, the confinement time, fusion power, helium fraction and power crossing the separatrix are determined. A number of confinement time scaling

laws are available in the module although the most commonly used is IPB98(y,2) [10]. The ratio of the effective helium confinement time (defined as the total helium content within the separatrix divided by the fusion rate) to the energy confinement time is generally chosen equal to 5, based on JET D-T experiments and extrapolations to ITER [11]. An important feature for this module is that only the power conducted and convected through the separatrix (P_{con}) is used in the confinement time scaling (not the total input power). Radiated powers are therefore excluded from the calculation of the IPB98 confinement scaling. One must bear in mind that the heating power is *not* an input to the plasma module. It is determined at the very end of the module by the plasma power balance.

Once the helium fraction is known, the alpha power is calculated:

$$P_\alpha = C_\alpha \frac{\langle n_e \rangle^2}{4} \overline{\sigma^* \nu_{DT}} E_\alpha V \tag{3}$$

where E_α is the alpha energy, V the plasma volume and $\overline{\sigma^* \nu_{DT}}$ the average fusion reaction rate coefficient. C_α is the dilution coefficient due to impurities (argon in the present case) and helium ash.

$$C_\alpha = \left(1 - 2f_{He} - Z_{Ar} f_{Ar}\right)^2 \tag{4}$$

The alpha power is then used to compute all the different β. The bootstrap fraction is then determined by a fit as described in [9]

$$f_{BS} = \frac{\beta_{p,th}}{A^{1/2}} \times 0.45 \sqrt{\frac{1 + \alpha_p^*}{1 + \alpha_j}} \tag{5}$$

where α_p^* is a thermal pressure peaking parameter and α_j an ad hoc current density peaking parameter.

Radiated powers are then calculated. The synchrotron power follows the scaling proposed in [12]. Line radiation is treated using an seeding impurity profile proportional to the electron density. This is a rough estimate as no simple way to compute impurity transport has yet been implemented in the plasma module. The total line radiation power is calculated using tabulated radiation coefficients from the ADAS database. Beryllium, argon and tungsten are available in the code but only argon is used at the moment. An important feature of the plasma module is that line radiation is considered as a loss for the total plasma power balance, up to a certain normalized radius ρ_{line}. A typical value is $\rho_{line} = 0.95$. This means than all the line radiation inside this radius will be considered as a power loss. This has significant consequences on the designs as addressed below in paragraph 3.1.3.

The plasma thermal balance is then closed with the additional heating power:

$$P_{add} = P_{con} + P_{Brem} + P_{synchro} + P_{linerad.} - P_{alpha} - P_{Ohmic} \tag{6}$$

The current driven by the amount of additional power calculated in equation is then given by

$$I_{CD} = \frac{\gamma_{CD}}{\langle n_e \rangle R} P_{add} = \frac{0.030 \times 10^{20} \langle T_e \rangle}{\langle n_e \rangle R} P_{add} \tag{7}$$

with Te in keV and n_e in m^{-3}.

The fit for γ_{CD} is only valid (strictly) for negative NBI current drive as stated in [9].

In cases where the current driven is larger to the plasma current set as input, the efficiency is artificially reduced. For steady-state designs where full non-inductive current drive is requested, situations where the power needed for thermal balance is lower than the one needed for current drive may occur. In this case, the mean temperature is increased (and the calculation restarted from the beginning to avoid inconsistencies) in order to increase the current drive efficiency. This increase is done up to a certain point in order not to deviate too much from the initial user input.

2.2. Divertor and edge module

Its main role is to compute the plasma temperature in the divertor and the heat flux on the targets. It also calculates the fuelling and pumping parameters in the divertor and scrape-off layer. Divertor target erosion is not taken into account in the present version of the module. It may be another limiting factor for the divertor and will be addressed in future versions of the code. The present version of the module takes as inputs the plasma geometry, safety factor at 95% flux, density at the separatrix, power conducted and convected through the separatrix (P_{con} in the previous section) and total radiated power from the plasma. Calculations are based on a basic two-point model [13] and only single-null divertor is considered in the present version. Calculations are applied to both inboard and outboard sides.

The scale length for power decay at the divertor target uses the following scaling law taken from [14]. More recent (and pessimistic) scalings have been recently implemented in the code [15], but their consequences on the power density are left for future work.

$$\lambda_q = 0.0031 \frac{2}{7} R \tag{8}$$

The parallel heat flux, considered as a constant along the field lines is calculated using the following formula:

$$q_{\parallel} = \frac{P_{con}}{4\pi a \lambda_q} q_{95} \tag{9}$$

The equations of the two-point model are then solved to get the target temperature T_t. f_{power} is the fraction of power lost in the Scrape-Off Layer (SOL). At this step of the calculation, f_{power} is only an assumption (a range of values between 0 and 1). The upstream density n_u is a user input. Typical values used in Sycomore are around $3.6.10^{19}$ m^{-3}.

$$\begin{cases} n_u T_u f_{mom} = 2 n_t T_t \\ T_u^{7/2} = T_t^{7/2} + \frac{7 f_{cond} q_\parallel L}{2\kappa_{0e}} \\ (1 - f_{power})\, q_\parallel) = \left(1 + \frac{\epsilon}{\gamma T_t}\right) \gamma \Gamma_t T_t \end{cases} \tag{10}$$

where κ_{0e} is the electron thermal conductivity, ϵ the mean energy lost per recycled neutral, γ is the sheath heat coefficient, Γ_t the particle flux on the target, f_{mom} a free parameter for momentum losses in the divertor and f_{cond} for conductive losses both set to 1.0 in the present version. f_{mom} will be computed consistently with the SOL parameters in a future version of the divertor module. Quantities with subscript u denote upstream values and subscript t target values. The upstream temperature T_u is then calculated with a conduction equation and density at the target is obtained using total pressure conservation.

The upstream temperature and density are used to compute the actual power lost in the SOL through impurity radiation (argon seeding in the present case). Equation 11 is the result of the heat balance between the upstream and the target points.

$$F_{Ar} = \left(\frac{f_{power} q_\parallel}{2 n_u \kappa_{0,e} T_{e,u}^2 \int_0^{T_{e,u}} \frac{1}{2} T_e^{0.5} L_Z(T_e) dT_e} \right)^2 \tag{11}$$

with $F_{Ar} = \frac{f_{Ar}}{Z_{eff}}$.
The argon fraction f_{Ar} can then be calculated.

$$f_{Ar} = \frac{F_{Ar}}{1 - 0.01 F_{Ar} Z_{Ar} (Z_{Ar} - 1)} \tag{12}$$

The integral term $\int_0^{T_{e,u}} \frac{1}{2} T_e^{0.5} L_Z(T_e) dT_e$ in equation 11 represents an impurity radiation loss function. It is calculated using interpolation of data presented in [16] and tabulated for argon in the code. It is to be noted that this integral assumes target temperature equal to zero. This speeds up calculation but tends to overestimate the radiation losses. Once equations 11 and 12 are established, the value of f_{power} corresponding to the argon fraction given in input can be determined.

The maximum heat flux on the inner/outer divertor target $q_{peak,in/out}$ is then computed:

$$q_{peak,in/out} = \frac{P_{con}(1 - f_{power}) - P_{rad,H}}{A_{wet,in/out}} f_{in/out} + \frac{f_{power} P_{con}}{A_{div}} f_{div} \tag{13}$$

$P_{rad,H} = e(\epsilon - E_i) n_t \sqrt{\frac{2eT_t}{m_i}} \frac{4\pi a \lambda_q}{q_{95}}$ is an hydrogen radiation term (ϵ is the cooling rate per injected neutral (25 eV) and E_i the ionization energy 13.6 eV). A_{wet} is the wetted area calculated using the divertor geometry, field lines angles (an input parameter in the present version) and an ad hoc flux expansion parameter. $f_{in/out}$ is the in/out power asymmetry factor (30% inboard, 60% outboard, 10% private region). f_{div} is the fraction of energy radiated in the SOL which ends on the divertor and A_{div} the total divertor

surface. The limiting heat flux considered for Sycomore calculations is the maximum of inner and outer q_{peak} values.

Once the heat flux is known, the argon fraction is adjusted to fulfill the constraint on the maximum heat flux on the divertor targets. This is done by a loop between the divertor module and the plasma physics module which computes the new plasma parameters taking into account the new argon fraction.

2.3. Blanket module

The present current blanket module treats only HCLL blankets. It is based on the HCLL design model described in [17]. The module computes the neutron flux from the fusion power provided by the plasma module. Then it calculates the breeding zone thickness needed to reach the breeding ratio specified by the user. Finally, the shield thickness is determined so that the peak fast neutron flux (> 0.1 MeV) reaching the inner leg of the toroidal field coil stays below a value set by the user. All components from blankets and shields (breeding zone, manifold, backplates, shields) are taken into account when calculating the neutron flux escaping from the blankets. The present module only uses fit functions derived from more advanced neutronics calculations. More refined neutronics using neural networks will be implemented in the near future [18, 19].

2.4. Magnet module

The magnet module is based on a simplified version of the ESCORT code [20]. The full derivation of the equations shown in the present section can be found in this reference. The magnet module in Sycomore takes as inputs the remaining space for TF and CS after other elements (plasma, first wall, blankets, shields and vacuum vessel) have been designed. It also takes a number of engineering parameters for the coils as inputs: number of TF coils, total current, magnetic field on axis, maximum allowable stress on TF and CS. It computes the conductor cross section needed to provide the requested magnetic field on axis, the equation derived from the expression of the centering stress and of the hoop stress to find the minimum size of the inner leg, such as presented in details in [20] .

In particular the expression of the average centering stress is the following:

$$\sigma_{centering} = \frac{2R_{e,TF}^2 \left(R_{e,TF} + 2R_{i,TF}\right) B_{maxTF}^2}{3\mu_0 R_{i,TF} \left(R_{e,TF} + R_{i,TF}\right)^2} \tag{14}$$

where $R_{e,TF}$ and $R_{i,TF}$ are respectively the external radius of the TF coil inner leg and the internal radius of the winding pack of the TF coil inner leg. B_{maxTF} is the maximum field on the conductor. The hoop stress term is presently taken as a constant (around 200 MPa) but will be calculated consistently as in [20] in future versions of the code. The hoop stress is a tension constraint and the centering stress is a compression constraint. The sum of these two stresses according to the Tresca criterion must stay

under 550 MPa in a conservative first approach; higher values will be used in the results presented below for a broader exploration.

The inboard sides of the TF coils (the nose) are wedged together to form a vault as described in [20]. The radial size of this vault is obtained by solving the equation determining the applied stress:

$$\sigma_{vault} = \frac{2\sigma_{centering} R_{i,TF}^2}{R_{i,TF}^2 - R_{I,vault}^2} \tag{15}$$

where $R_{i,vault}$ is the inner radius of the TF coil vault (and hence the inner radius of the whole TF coil structure assembly).

The central solenoid is designed by maximizing the available flux while fulfilling the constraint maximum hoop stress on the conductor steel. This stress is given by

$$\sigma_{hoopCS} = \frac{B_{CS}^2}{2\mu_0} f(R_{e,CS}/R_{i,CS}) \tag{16}$$

$R_{e,CS}$ and $R_{i,CS}$ are the external and internal radius of the central solenoid. $R_{e,CS}$ is obviously dependent on the internal radius of the TF vault which has been calculated just before. The full expression of function f can be found in appendix A of [20]. As the solenoid is multi-layered, the number of of layers is optimized such as yielding the maximum flux.

2.5. Plant power balance

The power balance module summarizes the power flows in the plant. It takes into account as sources the heat generated and absorbed by blankets and divertor. A constant user-defined energy multiplication factor is used in the present version. It will be determined by a neutronics module in the near future. Power sinks are the additional heating systems (with a user-defined wall-plug efficiency) blanket and divertor coolant pumping powers (helium in the present case) calculated using the temperatures currently assumed for commonly accepted HCLL designs. PbLi pumping power is also computed in a simple way (not taking into account the influence of the magnetic field) in the HCLL blanket case. Auxiliaries such as cryoplant are scaled up from ITER estimates as a first approximation. A fixed thermodynamical cycle efficiency is assumed. The module output is the net electric power to the grid.

2.6. Pulse duration

The burn duration Δt_{burn} is obtained from the following magnetic flux equation:

$$\Phi_{CS} = \Phi_{ramp-up} + V_{loop}\Delta t_{burn} = L_p I_p + C_{Ejima}\mu_0 R I_p + P_{ohm}\Delta t_{burn}/I_p \tag{17}$$

where L_p is the plasma total inductance. The flux available from the central solenoid Φ_{CS} is given by the magnet module and the ohmic power P_{ohm} by the plasma module.

The flux consumption at plasma breakdown as well as the contribution of the external poloidal coils to the available flux are neglected for the time being.

3. Applications to DEMO design

Sycomore was used to provide designs on two classes of tokamak reactors: pulsed machines and steady-state machines. These two classes are in line with the two main European concepts: DEMO1 (pulsed machine with conservative physics and technology) and DEMO2 (steady-state machine with advanced physics and technology).

3.1. Pulsed reactors

3.1.1. Design point. The optimization problem consists in designing a pulsed reactor of a minimum 500 MW net electric power and two hours burn duration for the smallest possible major radius. Input parameters, constraints and figures of merit are summarized in the first column of table 3.1.1. A population of 500 points and a tolerance of 5 cm on the converged optimum population is chosen for the genetic algorithm run. The optimum design found by the optimizer is summarized in tables 3.1.1 and 3.1.1 and. The inner radial build is also given on figure 3. The global design is in line with similar designs proposed by other system codes [21] with an aspect ratio of 3. One of the particular points of this design is the high NBI power needed to keep the plasma thermal balance. This is due to to the large line radiation power and will be addressed below in section 3.1.3. As a consequence, the H-mode threshold is largely met due to to the large power conducted and convected (P_{con}) through the separatrix. The net electric power fulfills the 500 MW constraint thanks to relatively optimistic NBI plug efficiency (>50%). Constraints on the TF coil steel stress have also been relaxed for this first study. This is due to the large total blanket and shield thickness required to protect the TF coil inner leg from excessive neutron damage. A large gap between plasma and magnets narrows down indeed the feasible domain for the TF coil inner leg.

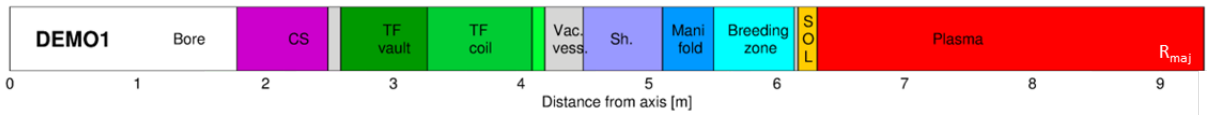

Figure 3. Inner radial build for DEMO1-like reactor (pulsed)

3.1.2. Sensitivity and operational domain. All the points explored by the genetic algorithm are stored during the search of the optimum. This gives a preliminary view of the width of the operational domain, although the mapping is neither necessarily exhaustive nor regular. The points indeed tend to converge towards the optimum rather than being spread over the entire parameter space. Figure 4 shows the net electric power achievable for different (R,a) designs tested in the course of the optimization run. The

	DEMO1
Figure of merit	Minimize R
Optimization variables	R, a, q_{95}, B_0
Constraints	
P_{net}	>500 MW
Flat-top duration	>7200 s
δ_{95}, κ_{95}	0.333, 1.518
Greenwald fraction f_{GW}	1.2
H-factor	1.1
NBI current drive efficiency	$0.03 \times \langle T_e \rangle$
Power flux to the divertor target	10 MW.m^{-2}
Tritium breeding ratio	1.1
Neutron flux on TF	10^{13} n.m^2.s^{-1}
Number of TF coils	18
Max. Stress on TF coil jacket	650 MPa
Max. Stress on TF coil vault	650 MPa
Max. Stress on CS coil	400 MPa

Table 1. Design constraints for DEMO1-like reactor (pulsed)

optimum lies in a region above R=9.5m and with some margin on the minor radius. One can notice that the area below a line defined by $R = 0.85a + 6.7$ (m) contains only invalid points. This corresponds to lack of space in the radial build. The transition is sharp, meaning that designs too close to this boundary have little margin on the radial build. Other invalid points in the rest of the operational space correspond to too high toroidal fields invaliding the TF coil design or too high power crossing the separatrix (meaning that the edge plasma lies outside usual physics regimes).

Figure 5 displays the net electric power as a function of the pulse duration of different major radii. It shows that a trade-off between pulse duration and electric power has to be found for a given major radius. Increasing the net electric output to the 800 MW range is feasible with moderate major radius increase only if the pulse duration is short enough. Increasing the power on designs with more than 10 hours burn time becomes very costly in major radius: $R \approx 10$m is needed for designs with 2 hours burn whereas more than 12 m are needed for designs with 20 hours. This also shows that the validity domain for long pulse machines with more than 500 MW net electric power narrows down with the pulse duration. 40 hours pulsed machines with 500 MW leave little margin on the available space. It is to be noted that because of the high additional power needed to compensate the radiation losses in these designs, the current drive power is also large. This explains the possibility to get design points with more than 10 hours burn duration. Most of the points below 500 MW net electric power are actually steady-state reactors for the same reason. However, the large recirculating

Results	DEMO1
R/a	9.34 m/3.025 m
I_p	20.57 MA
B_t	5.99 T
q_{95}	3.17
Boostrap fraction	29%
NBI-drived current	68%
τ_E	3.87 s
Thermal energy content	1461 MJ
β_N	2.58
Z_{eff}	3.09
Helium concentration	7.2%
Argon concentration	0.63%
$\langle n_e \rangle$	8.03×10^{19} m^{-3}
$\langle T_e \rangle$	14.38 keV
$n_{e,max,ped,edge}$	9.6, 7.36, 3.6×10^{19} m^{-3}
$T_{e,max,ped,edge}$	36.1 keV, 2.20 keV, 0.1 keV
P_{fus}	2218 MW
P_{brem}	111 MW
P_{synch}	61 MW
P_{line}	165 MW
P_{con}	337 MW
P_{NBI}	251 MW
$P_{L-Hthresh.}$	142 MW
Q	8.83
$P_{Hepumping}$	238 MW
P_{cryo}	34 MW
$P_{net,elec}$	526 MW
Flux from CS	378 Wb
Burn duration	7200 s

Table 2. Design result for DEMO1-like reactor (pulsed)

power needed for high auxiliary powers might be a concern from the economic point of view as the cost of infrastructures to handle such high powers is likely to be an issue. The number of access ports for heating systems might also decrease the space available for blankets. These points are possible midterm upgrades for Sycomore's calculations.

A more systematic scan of the parameter space was done by a random sampling of the optimization variables (R, a, Bt, q_95). Random sampling algorithms are indeed available within the URANIE framework. A first rough scans of 10^5 points (figure 6) confirms that no valid points are found below 9 m major radius or for too low aspect

Element	radial size
Central bore	1.77 m
CS coil	0.72 m
TF coil internal casing	0.1 m
TF coil vault	0.68 m
TF coil	0.82 cm
TF coil external casing	0.1 m
Vacuum vessel	0.3 m
Shield	0.62 m
Manifold	0.4 m
Breeding zone	0.63 m
First wall	0.03 m
SOL	0.15 m
Plasma radius	3.025 m

Table 3. Inner radial build for DEMO1-like reactor (pulsed)

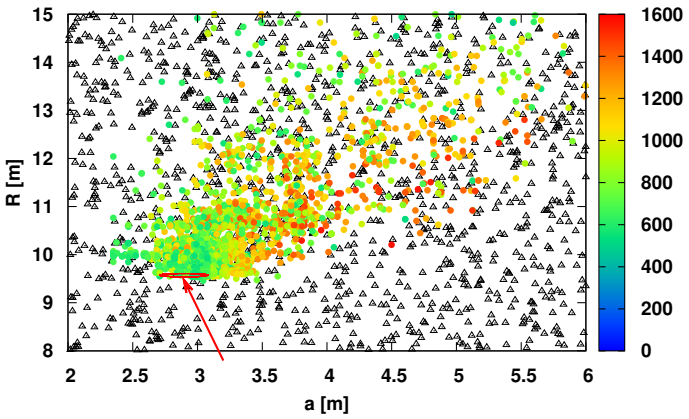

Figure 4. Pulsed DEMO. Net electric power map in (R,a) space. Black triangles are invalid design points (e.g. lack of space in radial build). The optimum zone is pointed out by the arrow.

ratios. Sampling the space closer to the optimum previously found confirms its location around (R,a)=9.3m/3.025m as shown on figure 7(a). The map of net electric power as a function of burn duration for different major radii is shown on figure 7(b) and confirms the trends highlighted by figure 5: increasing the net electric power is more expensive for long burns.

3.1.3. Treatment of line radiation power. As mentioned in the design summary, most of the pulsed reactor designs found by Sycomore need high auxiliary heating powers

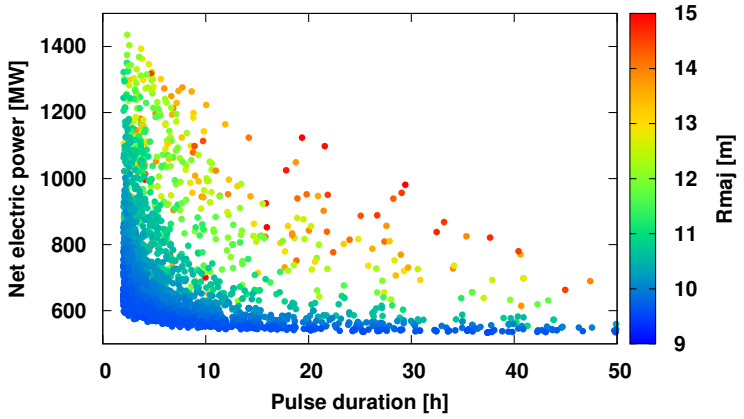

Figure 5. Pulsed DEMO. Net electric power as a function of pulse duration for different major radiuses

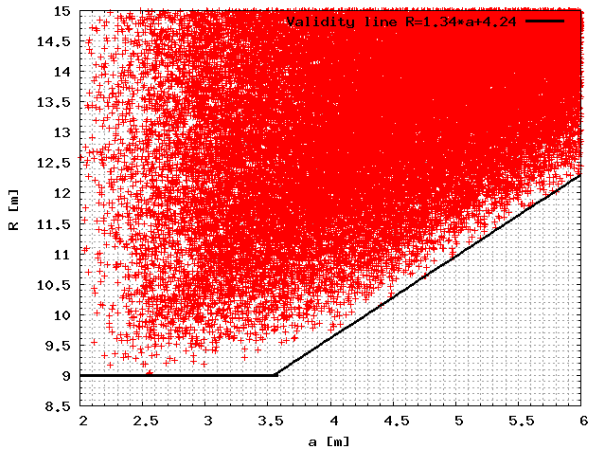

Figure 6. Pulsed DEMO. Valid design points obtained from a random sampling of the parameter space.

(around 200 MW). This is due to the line radiation treatment in the plasma module. Conversely to bremsstrahlung and synchrotron powers which are predominantly located in the plasma core, line radiation (of argon in present cases) occurs near the edge and pedestal. Sycomore defines a minor radius ρ_{line} within which the line radiated power is accounted as a loss. Line radiation power outside this radius is not taken into account in the plasma power balance. The present ρ_{line} is at the pedestal radius. As shown on figure 8(a) for a fixed design, a significant part of the line radiated power is radiated inside the core zone limited by the pedestal radius. This represents a major loss term for the plasma power balance. The minor radius within which P_{line} is no longer considered as a loss (ρ_{line}) has a major effect on the NBI power needed in the power balance as

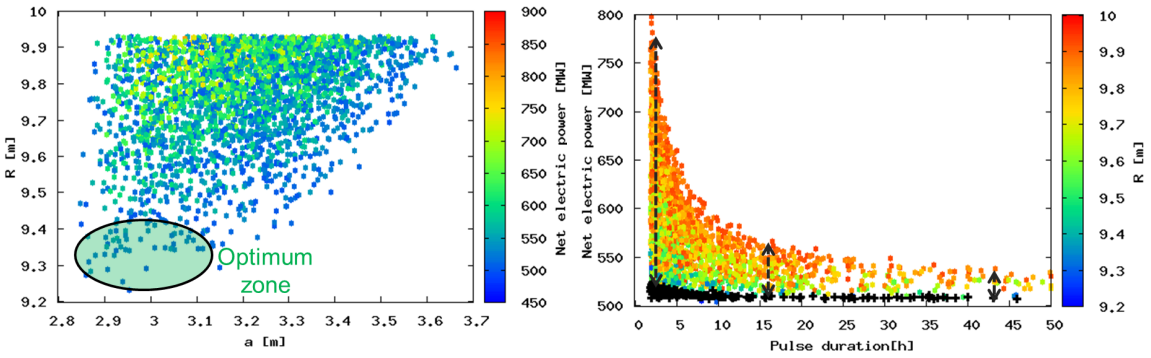

Figure 7. Pulsed DEMO. (a) Net electric power map in (R,a) space mapped by random sampling. (b) Net electric power as a function of pulse duration for different major radii. Black points are the optimum population.

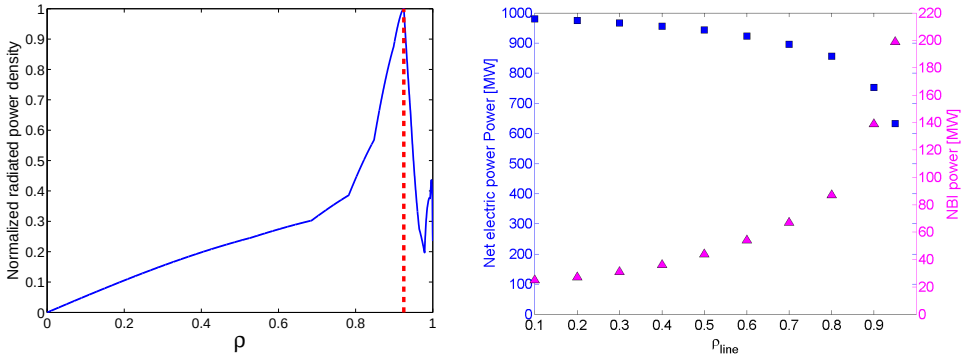

Figure 8. (a)Normalized radiated power density along normalized radius. Dashed line indicates pedestal. - (b)$P_{net,elec}$ output as a function of ρ_{line}

shown on figure 8(b). High NBI power also leads to high power going through the separatrix, explaining the high P_{con}/R values obtained in those designs compared to other codes. The treatment of line radiation should therefore be refined in order to reduce uncertainties in system codes.

3.2. Steady-state reactors

3.2.1. Design point. Sycomore was used to provide a design for a steady-state reactor. The optimization scenario is given in table 3.2.1 (left). The aim of the optimization problem was to get the smallest major radius for a 500 MW net electric power reactor. This design is more advanced than the pulsed reactor as it assumes a higher H-factor, higher elongation and assumes that a fully non-inductive current drive scenario is used. All other constraints remain the same as for the pulsed design. As expected and shown on tables 3.2.1 and 3.2.1, the machine is more compact due to the better confinement and the less severe constraints on the central solenoid. The plasma current is also lowered as it is favorable from the power needed for current drive. The inner radial build is given on figure 9. Better confinement also means that less power is conducted and convected through the separatrix, calling for lower heat loads on the divertor, lower argon seeding fraction and hence lower line radiated power than the pulsed DEMO1 design.

	DEMO2
Figure of merit	Minimize R
Optimization variables	R, a, q_{95}, B_0
Constraints	
P_{net}	>500 MW
Flat-top duration	∞
δ_{95}, κ_{95}	0.333, 1.604
Greenwald fraction f_{GW}	1.2
H-factor	1.4
NBI current drive efficiency	$0.03 \times \langle T_e \rangle$
Power flux to the divertor target	10 MW.m^{-2}
Tritium breeding ratio	1.1
Neutron flux on TF	10^{13} n.m^2.s^{-1}
Number of TF coils	18
Max. stress on TF coil jacket	650 MPa
Max. stress on TF coil vault	650 MPa
Stress on CS coil	400 MPa

Table 4. Design constraints for DEMO2-like reactor (steady-state)

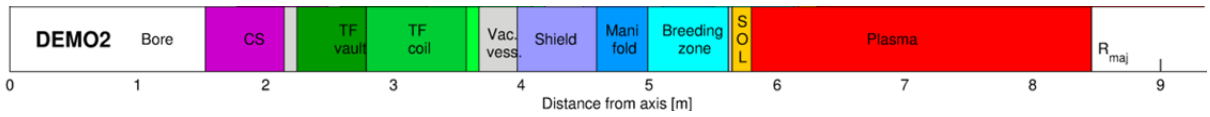

Figure 9. Inner radial build for DEMO2-like reactor (steady-state)

3.2.2. Sensitivity. Figure 10 shows a map of the net electric power as a function of (R, a). A relatively broad zone of net electric power close to 500 MW is found around (R,a) = (8.7m,2.7m). Increasing the major radius to allow more margin in the radial build is possible at the cost of a slow reduction of the net electric power output. Conversely, the line ($R = 1.1a + 5.4$ (m)) which defines the boundary for most compact machines is much sharper: all points located below this boundary are invalid due to the radial build check. The smaller offset of this line equation compared to the same one for the pulsed DEMO1 design is due to the reduced size of the central solenoid. One has to note that this boundary prevents the increase of minor radius without increasing significantly the major radius ($R \geq 10.5m$ for $P_{net,elc} \geq 800MW$). Increasing the net electric power is more expensive in terms of major radius increase for this range of steady-state designs than for pulsed designs. At least 11 m major radius is needed to get a reliable (i.e. not on the edge of the operational domain) 800 MW steady-state design point, to be compared with 9.5 m to 10 m needed for pulsed designs. This is due to the power needed for current drive in large machines with large plasma currents,

Results	DEMO2
R/a	8.46 m/2.66 m
I_p	15.69 MA
B_t	5.53 T
q_{95}	3.43
Boostrap fraction	41%
NBI-drived current	59%
τ_E	3.55 s
Thermal energy content	1105 MJ
β_N	3.43
Z_{eff}	2.73
Helium concentration	7.3%
Argon concentration	0.52%
$\langle\ n_e\ \rangle$	7.94×10^{19} m^{-3}
$\langle\ T_e\ \rangle$	15.16 keV
$n_{e,max,ped,edge}$	9.44, 7.26, 3.6×10^{19} m^{-3}
$T_{e,max,ped,edge}$	38 keV, 2.32 keV, 0.1 keV
P_{fus}	1734 MW
P_{brem}	71 MW
P_{synch}	43 MW
P_{line}	91 MW
P_{con}	289 MW
P_{NBI}	143 MW
Q	12.52
$P_{Hepumping}$	187 MW
P_{cryo}	27 MW
$P_{net,elec}$	496 MW
Flux from CS	270 Wb
Burn duration	∞

Table 5. Design results for DEMO2-like reactor (steady-state)

which calls for larger machine to keep a high enough net electric output.

Conclusion and discussion

Sycomore is a modular system code aimed at providing consistent DEMO designs taking into account simple models to describe all the major elements of a fusion reactor. It has been implemented as a fully modular, explicit workflow under the ITM platform. The present version of the code contains modules for the following elements: plasma, divertor, tritium breeding blanket, TF shield, TF coils, CS coil, plant power balance and

Element	radial size
Central bore	1.53 m
CS coil	0.62 m
TF coil internal casing	0.1 m
TF coil vault	0.54 m
TF coil	0.78 cm
TF coil external casing	0.1 m
Vacuum vessel	0.3 m
Shield	0.62 m
Manifold	0.4 m
Breeding zone	0.63 m
First wall	0.03 m
SOL	0.15 m
Plasma radius	2.66 m

Table 6. Inner radial build for DEMO2-like reactor (pulsed)

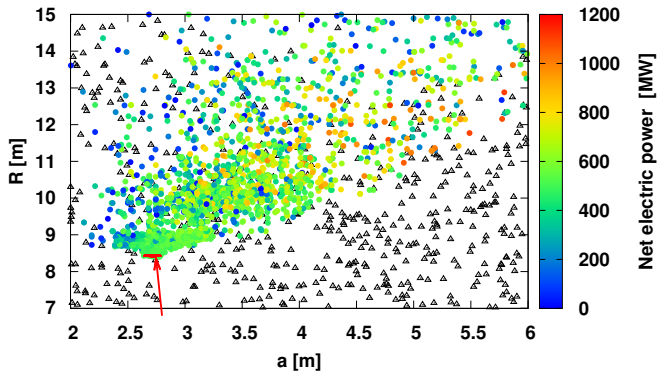

Figure 10. $P_{net,elec}$ map in (R,a) for steady-state designs. Optimum solution zone is pointed out by the red arrow. Black triangles are invalid designs (e.g. lack of space in radial build)

pulse duration. It is coupled to an optimization platform to be able to specify figures of merit and constraints for a design study. Both pulsed and steady-state designs can be obtained with Sycomore. The design consistency enforced along the calculation chain allows quick analysis of design points and the external optimization framework allows flexibility in sensitivity studies and parameter space exploration. Sycomore thus combines the advantages of direct codes [1] providing optimized designs for a set of inputs and codes using large databases [2] to map the parameter space.

Results are presented on both pulsed and steady-state designs. A pulsed reactor (DEMO1-like) with 500 MW net electric power and 2 hours burn durations is described, in line with results obtained by other system codes. Sycomore highlights that longer burn durations only exist in a very narrow operational domain. The design is sensitive to

the treatment of line radiation power. A smaller steady-state advanced tokamak design is also presented. It is also shown that increasing the net electric power above 800 MW requires a larger major radius increase for steady-state designs than for short-burn ($\sim$ 2 hours) pulsed designs. More advanced multi-criterion sensitivity studies are planned in the near future for Sycomore. New modules are also being implemented to extend the code capabilities.

Acknowledgments

This work has been carried out within the framework of the EUROfusion Consortium and has received funding from the European Unions Horizon 2020 research and innovation programme under grant agreement number 633053. The views and opinions expressed herein do not necessarily reflect those of the European Commission.

[1] M. Kovari, R. Kemp, H. Lux, P. Knight, J. Morris, and D.J. Ward. process: A systems code for fusion power plantspart 1: Physics. *Fusion Engineering and Design*, 89(12):3054 – 3069, 2014.

[2] Zoran Dragojlovic, A. Rene Raffray, Farrokh Najmabadi, Charles Kessel, Lester Waganer, Laila El-Guebaly, and Leslie Bromberg. An advanced computational algorithm for systems analysis of tokamak power plants. *Fusion Engineering and Design*, 85(2):243 – 265, 2010.

[3] Makoto Nakamura, Richard Kemp, Hiroyasu Utoh, David J. Ward, Kenji Tobita, Ryoji Hiwatari, and Gianfranco Federici. Efforts towards improvement of systems codes for the broader approach {DEMO} design. *Fusion Engineering and Design*, 87(56):864 – 867, 2012. Tenth International Symposium on Fusion Nuclear Technology (ISFNT-10).

[4] G.L. Falchetto, D. Coster, R. Coelho, B.D. Scott, L. Figini, D. Kalupin, E. Nardon, S. Nowak, L.L. Alves, J.F. Artaud, V. Basiuk, Joo P.S. Bizarro, C. Boulbe, A. Dinklage, D. Farina, B. Faugeras, J. Ferreira, A. Figueiredo, Ph. Huynh, F. Imbeaux, I. Ivanova-Stanik, T. Jonsson, H.-J. Klingshirn, C. Konz, A. Kus, N.B. Marushchenko, G. Pereverzev, M. Owsiak, E. Poli, Y. Peysson, R. Reimer, J. Signoret, O. Sauter, R. Stankiewicz, P. Strand, I. Voitsekhovitch, E. Westerhof, T. Zok, W. Zwingmann, ITM-TF Contributors, the ASDEX Upgrade Team, and JET-EFDA Contributors. The european integrated tokamak modelling {ITM} effort: achievements and first physics results. *Nuclear Fusion*, 54(4):043018, 2014.

[5] I. Altintas, C. Berkley, E. Jaeger, M. Jones, B. Ludascher, and S. Mock. Kepler: an extensible system for design and execution of scientific workflows. In *Scientific and Statistical Database Management, 2004. Proceedings. 16th International Conference on*, pages 423–424, June 2004.

[6] Fabrice Gaudier. Uranie: The cea/den uncertainty and sensitivity platform. *Procedia - Social and Behavioral Sciences*, 2(6):7660 – 7661, 2010. Sixth International Conference on Sensitivity Analysis of Model Output.

[7] Rene Brun and Fons Rademakers. {ROOT} an object oriented data analysis framework. *Nuclear Instruments and Methods in Physics Research Section A: Accelerators, Spectrometers, Detectors and Associated Equipment*, 389(12):81 – 86, 1997. New Computing Techniques in Physics Research V.

[8] G. Arnaud. Manuel d'utilisation de vizir distribu v2.0; rapport cea sfme/lgls/rt/10-001/a, october 2009.

[9] J. Johner. Helios: A zero-dimensional tool for next step and reactor studies. *Fusion Science and Technology*, 59(2):308–349, 2011.

[10] ITER Physics Expert Group on Confinement and Transport and Confinement Modelling and Database and ITER Physics Basis Editors. Chapter 2: Plasma confinement and transport. *Nuclear Fusion*, 39(12):2175, 1999.

[11] A. Loarte, B. Lipschultz, A.S. Kukushkin, G.F. Matthews, P.C. Stangeby, N. Asakura, G.F. Counsell, G. Federici, A. Kallenbach, K. Krieger, A. Mahdavi, V. Philipps, D. Reiter, J. Roth, J. Strachan, D. Whyte, R. Doerner, T. Eich, W. Fundamenski, A. Herrmann, M. Fenstermacher, P. Ghendrih, M. Groth, A. Kirschner, S. Konoshima, B. LaBombard, P. Lang, A.W. Leonard, P. Monier-Garbet, R. Neu, H. Pacher, B. Pegourie, R.A. Pitts, S. Takamura, J. Terry, E. Tsitrone, and the ITPA Scrape-off Layer and Divertor Physics Topical Group. Progress in the ITER Physics Basis Chapter 4: Power and particle control. *Nuclear Fusion*, 47(6):S203, 2007.

[12] F. Albajar, J. Johner, and G. Granata. Improved calculation of synchrotron radiation losses in realistic tokamak plasmas. *Nuclear Fusion*, 41(6):665, 2001.

[13] P. Stangeby. *The Plasma Boundary of Magnetic Fusion Devices*. Institute of Physics Publishing, 2000.

[14] A. Kallenbach, N. Asakura, A. Kirk, A. Korotkov, M.A. Mahdavi, D. Mossessian, and G.D. Porter. Multi-machine comparisons of h-mode separatrix densities and edge profile behaviour in the itpa sol and divertor physics topical group. *Journal of Nuclear Materials*, 337339(0):381 – 385, 2005. PSI-16.

[15] T. Eich, A.W. Leonard, R.A. Pitts, W. Fundamenski, R.J. Goldston, T.K. Gray, A. Herrmann, A. Kirk, A. Kallenbach, O. Kardaun, A.S. Kukushkin, B. LaBombard, R. Maingi, M.A. Makowski, A. Scarabosio, B. Sieglin, J. Terry, A. Thornton, ASDEX Upgrade Team, and JET EFDA Contributors. Scaling of the tokamak near the scrape-off layer h-mode power width and implications for iter. *Nuclear Fusion*, 53(9):093031, 2013.

[16] D. Post, N. Putvinskaya, F.W. Perkins, and W. Nevins. Analytic criteria for power exhaust in divertors due to impurity radiation. *Journal of Nuclear Materials*, 220222(0):1014 – 1018, 1995. Plasma-Surface Interactions in Controlled Fusion Devices.

[17] A. Li-Puma, J. Bonnemason, L. Cachon, J.L. Duchateau, and F. Gabriel. Consistent integration in preparing the helium cooled lithium lead demo-2007 reactor. *Fusion Engineering and Design*, 84(711):1197 – 1205, 2009. Proceeding of the 25th Symposium on Fusion Technology (SOFT-25).

[18] J.-C. Jaboulay, A. Li Puma, and J. Martnez Arroyo. Neutronic predesign tool for fusion power reactors system assessment. *Fusion Engineering and Design*, 88(910):2336 – 2342, 2013. Proceedings of the 27th Symposium On Fusion Technology (SOFT-27); Lige, Belgium, September 24-28, 2012.

[19] Antonella Li-Puma, Jean-Charles Jaboulay, and Brunella Martin. Development of the breeding blanket and shield model for the fusion power reactors system {SYCOMORE}. *Fusion Engineering and Design*, 89(78):1195 – 1200, 2014. Proceedings of the 11th International Symposium on Fusion Nuclear Technology-11 (ISFNT-11) Barcelona, Spain, 15-20 September, 2013.

[20] J.-L. Duchateau, P. Hertout, B. Saoutic, J.-F. Artaud, L. Zani, and C. Reux. Conceptual integrated approach for the magnet system of a tokamak reactor. *Fusion Engineering and Design*, 89(11):2606 – 2620, 2014.

[21] G. Federici, R. Kemp, D. Ward, C. Bachmann, T. Franke, S. Gonzalez, C. Lowry, M. Gadomska, J. Harman, B. Meszaros, C. Morlock, F. Romanelli, and R. Wenninger. Overview of eu demo design and r& d activities. *Fusion Engineering and Design*, 89(78):882 – 889, 2014. Proceedings of the 11th International Symposium on Fusion Nuclear Technology-11 (ISFNT-11) Barcelona, Spain, 15-20 September, 2013.